Chinese Chemical Letters 34 (2023) 107448

Contents lists available at ScienceDirect

Chinese Chemical Letters

journal homepage: www.elsevier.com/locate/cclet

Delivery of MicroRNAs by plant virus-based nanoparticles to functionally alter the osteogenic differentiation of human mesenchymal stem cells

Fei Xue[a], Jeroen J.L.M. Cornelissen[b], Quan Yuan[a,*], Shuqin Cao[a,*]

[a] State Key Laboratory of Oral Diseases, West China Hospital of Stomatology, Sichuan University, Chengdu 610041, China
[b] Department of Molecules & Materials, MESA+ Institute for Nanotechnology, University of Twente, Enschede AE 7500, the Netherlands

ARTICLE INFO

Article history:
Received 2 December 2021
Revised 15 April 2022
Accepted 19 April 2022
Available online 22 April 2022

Keywords:
VLPs
Cowpea chlorotic mottle virus
Gene delivery
MicroRNAs
Osteogenesis

ABSTRACT

MicroRNA-26a (miR-26a) has been verified to promote osteogenic differentiation of mesenchymal stem cells in recent years. The main obstacles to its application in bone regeneration are instability in the physiological environment and low efficiency of cellular membrane penetration. To overcome these problems, we constructed a novel plant virus gene delivery system based on Cowpea chlorotic mottle virus (CCMV). By encapsulating miR-26a with purified capsid protein (CP) dimers derived from CCMV, CP-miR-26a (CP26a) virus-like particles (VLPs) were obtained. CP26a retained a structure similar to the native CCMV and protected miR-26a from digestion with its exterior CP. Moreover, CP26a featured similar cellular uptake efficiency, osteogenesis promotion ability, and better biocompatibility compared with Lipofectamine2000-miR-26a (lipo26a), which indicated a promising prospect for CCMV as a novel gene delivery system.

Treatment of bone defects due to trauma, tumor, inflammation, *etc*. is a major challenge from the standpoints of clinical and socioeconomic perspectives. To date, autogenous bone grafts are still the gold standard and most considered therapeutic strategy due to their remarkable osteoconductive and osteoinductive properties [1], albeit drawbacks such as the limited amount of donor tissue, excessive harvest procedure, and the possibility of postoperative infection of the donor site [2]. Alternatively, xenogeneic bone graft materials represented by bovine-derived bone materials are widely used in clinics despite their limitations including inflammatory response, quick absorption rate, and obstacles in modification [3,4]. Therefore, it is necessary to pursue high-efficiency and bio-safe bone regeneration materials.

Biomaterials that mimic the structural, mechanical, and biological properties of natural tissues have been attracting significant attention [5–8]. Meaningful progress has been made in designing and fabricating new materials to properly address cell activity. For example, ROS-PAMAM could assist siRNA release in the tumor environment [9], PEI-FeOOH facilitated siRNA delivery in the cancer cell to induce gene silencing [10], nano assembly HA-ADA/TEPA-CD served as a pDNA container and achieved controlled release [11]. For bone regeneration biomaterials, one of the commonly used methods is to incorporate biologically active molecules such as growth factors [12,13], bioactive peptides [14], and nucleic acids [15,16]. MicroRNAs (miRNAs) are highly conserved noncoding small RNAs consisting of 20–23 nucleotides, they can interact with target sites present in the 3′-untranslated regions (UTR) of specific mRNAs. MiRNAs represent an important class of transcriptional modulators for both fine-tuning and dramatically altering cell behavior by inducing degradation of targeted mRNA and inhibition of translating process, and it is believed that miRNAs control the activity of 60% of all protein-coding genes in humans [17]. For example, MicroRNA-26a (miR-26a), which has been verified to specifically inhibit GSK-3β protein, subsequently inhibit β-catenin phosphorylation and activate Wnt signaling pathway to promote osteogenic differentiation of MSCs, thereby induce osteogenic differentiation process *in vitro* [18–20]. Nonetheless, being negatively charged, miRNAs cannot easily penetrate the cell membranes. And it tends to biodegrade *in vivo*. To overcome these, Liu *et al*. [21] reported that lentivirus-mediated miR-26a overexpression in BMSC could promote the regeneration of mouse calvaria bone defects. However, biosafety and host immune response caused by lentivirus-based transfection limited its application. Synthetic gene delivery systems such as liposome vesicles and high molecular weight polyethylenimine (PEI) are be-

* Corresponding authors.
E-mail addresses: yuanquan@scu.edu.cn (Q. Yuan), caoshuqin2020scu@foxmail.com (S. Cao).

https://doi.org/10.1016/j.cclet.2022.04.046
1001-8417/

ing widely used due to their good transfection efficiency, Zhang *et al.* [16] developed a novel cell-free scaffold, which featured with two-stage delivery of miR-26a to repair critical-sized calvaria defects. The hyperbranched polyesters formed "double shell" polyplexes and then were encapsulated into PLGA microspheres. PLGA microsphere was then immobilized on a poly(L-lactic acid) (PLLA) scaffold. The PLLA scaffold exhibited long-term release of miR-26a, high transfection efficiency, and capability of regenerating critical-sized calvarial bone defects both in healthy and osteoporotic mice; Yan *et al.* [20] applied PEI and KALA decorated mesoporous silica nanoparticles (MSNs) to deliver miR-26a. MSN_miR-26a@PEI-KALA nanoparticles could protect miR-26a from degradation and promote rBMSCs osteogenic differentiation *in vitro* efficiently; however, their biocompatibility would be a major concern for regenerative therapy. Recently, many studies focused on exploring the possibility of plant virus as a gene delivery system and made promising progress. Tobacco mosaic virus (TMV) has been experimentally applied in targeted delivery to tumor cells such as melanoma [22], breast cancer cells [23], and ovarian tumor cells [24]. Cowpea mosaic virus (CPMV) can also be modified chemically for dual delivery to macrophages and cancer cells [25]. Cowpea chlorotic mottle virus (CCMV), a single-stranded RNA plant virus with the structure of regular icosahedron of 28 nm diameter, has also been reported. CCMV could be stable *in vitro* and protect its nucleotide from degradation [26].

CCMV can disassemble and reassemble under different ion concentrations and pH conditions, which facilitates its application as a nucleotide delivery platform [27]. When CCMV was disassembled and its native RNA genome was removed, the purified positive charged capsid protein (CP) could be obtained to encapsulate various cargoes. For example, CCMV has been confirmed to deliver siRNA and downregulate gene expression [28], improve the antitumor efficacy of CpG oligonucleotides [29]. Moreover, the enhanced green fluorescent protein (EGFP) has been successfully encapsulated by CP with noncovalent binding [30]. Among various gene vectors, the superiority of plant virus is better biocompatibility and acceptable efficiency [31,32]. At present, a mature protocol to disassemble CCMV, remove its native RNA genome, and obtain purified CP components has been established.

Based on the above, we used virus-like particles (VLPs) derived from CCMV, to carry miR-26a, into human mesenchymal stem cells (hMSCs) to promote the osteogenesis process *in vitro*. By adjusting the pH and ion concentration, we removed the native RNA of CCMV to obtain CP and successfully encapsulated the miR-26a with them. Compared with the traditional gene vector Lipofectamine2000 reagent, the CP26a VLPs exhibited satisfactory biocompatibility and comparative delivery efficiency as well as osteogenesis ability. Thus, there is great promise for CCMV to be developed and applied in short-stranded nucleic acid delivery therapy *in vitro*.

CCMV was replicated by inoculation of the cowpea leaves and extracted by PEG precipitation, density gradient centrifugation in which CCMV suspension was mixed with cesium chloride. The removal of native viral genomic RNA was performed by dialysis in RNA buffer and cleaning buffer in turn and long-hour, high-speed centrifugation [33]. Then CPs were dialyzed into a 5x assembly buffer to maintain their form of protein dimer. To encapsulate miRNAs, miR-26a and CP were mixed at a 6:1 (w/w) ratio and reassembled in the buffer with low pH and the presence of Mg^{2+} (Scheme 1) [23].

Agarose gel electrophoresis assay was used to confirm the successful preparation of CP26a. Fig. 1A revealed that the migration of CP26a was distinctly lower than naked miR-26a. Furthermore, the image of the gel stained with coomassie bright blue dye indicated a co-localization of nucleotide with protein in the lane of the CP26a sample. The results could be explained by charge density

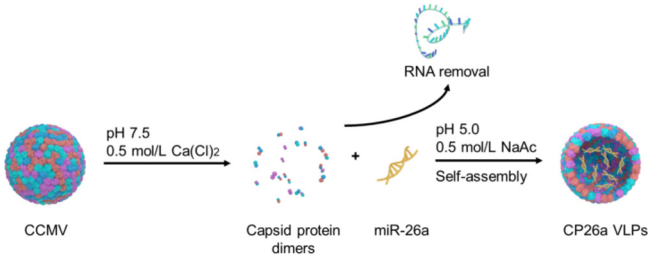

Scheme 1. CCMV disassembly and CP26a VLPs preparation strategy. CCMV was disassembled in RNA removal buffer to obtain CP, then miR-26a was encapsulated with CP at lower pH.

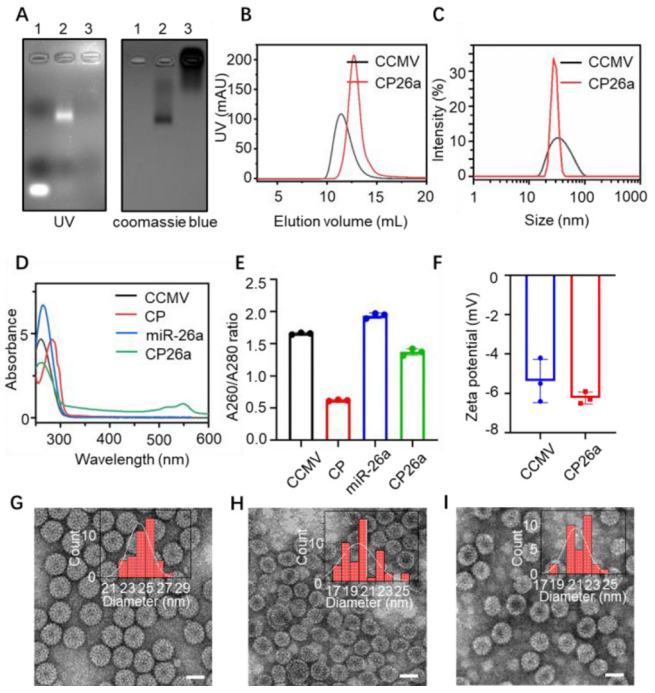

Fig. 1. Physicochemical characteristics of CP26a *versus* CCMV, CP, and miR-26a. (A) Nucleotides (left) and protein (right) detection of miR-26a (Lane1), CP26a VLPs (Lane 2), and CP dimers (Lane 3) by agarose gel electrophoresis. (B) FPLC analysis of CCMV and CP26a. (C) DLS analysis of CCMV and CP26a. (D) UV–vis absorbance spectrophotometry detection of CCMV, CP, miR-26a, and CP26a. (E) A260/A280 ratio of CCMV, CP, miR-26a, and CP26a. (F) Zeta potential detection of CCMV and CP26a VLPs. TEM images and size statistics of CCMV (G), CP26a (H), and CP26a 15 days after preparation (I). (Scale bar= 20 nm).

change due to VLPs formation. Particularly, the pure CPs sample stayed around the electrophoresis starting point near the negative field, which could be caused by the absence of negative charge due to the removal of native viral genomic RNA [32].

After the successful encapsulation, CP26a was purified by FPLC, and the individual peak exhibited the satisfactory structural integrity of VLPs with no significant CP dimers nor naked miRNAs (Fig. 1B). Meanwhile, the elution volume of CP26a was ~12.5 mL while that of CCMV was ~11 mL, which might indicate that CP26a is smaller than native CCMV.

To further investigate the structure difference between CP26a and CCMV, DLS, UV–vis spectrometer, and zeta potential experiments were carried out. DLS measurement indicated the diameter of CP26a was 27.1 ± 3.5 nm, PDI as 0.017, whereas that of native CCMV was 33.7 ± 14 nm, PDI as 0.039 (Fig. 1C). UV–vis absorbance spectrophotometry showed a similar spectrum of CP26a and CCMV (Fig. 1D). The A260/A280 ratio of CP26a was 1.37, which was similar to the native CCMV particles (1.66). In contrast, the ra-

tio of CP dimers was 0.62, indicating the complete removal of native viral ssRNA. The variation from 0.62 to 1.37 indicated the successful encapsulation of miR-26a (Fig. 1E). No significant change in the electric potential of CP26a was found as that of CP26a and CCMV were -6.23 ± 0.25 mV and -5.37 ± 0.90 mV respectively (Fig. 1F). In terms of microscopic morphology, TEM revealed that both native CCMV and CP26a were uniform and regular spherical nanoparticles. We counted particle size and found that the distribution of CCMV ranged from 22∼28 nm while that of CP26a in the range of 17∼26 nm (Figs. 1G and H). Researchers have studied the resemble structure of VLPs derived from CCMV with cryo-EM, there they claimed that CCMV-CP remained intrinsic structure when assembled with negatively charged polymers, RNA, or DNA [34]. Furthermore, Stan *et al.* [35] have demonstrated that the minimal length required for the assembly of VLPs is 14 nucleotides. In our experiment, 22 bp dsRNA was applied to form VLP. Therefore, we claimed that the VLPs featured a similar structure to native CCMV.

Finally, the quantity of nucleic acid encapsulated in CP26a was measured by UV–vis absorbance spectrophotometry (Fig. S1 in Supporting information). To facilitate the quantification, CY3 was used to functionalize miR-26a at its 5′. Then the concentration of loaded miR-26a was calculated *via* standard curve as 100∼150 μg/mL (5.7∼8.6 μmol/L), 0.186 (w/w) of miR-26a/CP weight ratio. It can be deduced that each CP cage packed about 16 double-stranded miR-26a. This disassembly and reassembly approach is therefore a rapid and efficient way to prepare CP26a.

To further verify the stability of CP26a after preparation, FPLC, DLS, and TEM were used to study the composition and morphology change of CP26a at 7, 15, and 30 days after preparation. Both TEM and statistical analysis (Fig. 1I) indicated the uniform size of CP26a nanoparticles at 15-days after preparation. According to the DLS study (Fig. S2B), the size of CP26a was around 27.8 ± 5.3 nm with a relatively low PDI value (0.057). Furthermore, FPLC (Fig. S2A in Supporting information) results showed that CP26a samples were eluted at elution volume $V \approx 12.5$ mL, and no monomers were eluted out (supposed elution volume: 18.5 mL) indicating that CP26a retained its assembled structure at 15 days after preparation. What is more, DLS and TEM data of CP26a indicated that CP26a remained its uniform size (Fig. S2D in Supporting information) even 30 days after preparation. The diameter statistics also revealed a narrow distribution (PDI: 0.056). The results above suggested that miR-26a encapsulated VLPs were stable under *in vitro* circumstances within one month, this might expand the application of miRNAs.

To investigate the cellular uptake efficiency of hMSCs to CP26a, we co-cultured hMSCs with CCMV-Atto647 (CCMV surface decorated with Atto647 fluorescence), CP26a-CY3 (CP encapsulated miR-26a decorated with CY3 at 5′), and lipo26a-CY3 (liposome complex encapsulated miR-26a decorated with CY3 at 5′), respectively. Fluorescence microscope images showed that most hMSCs were Atto647/CY3-positive cells, and red fluorescence localization was constrained within the cytoplasm (Fig. 2A). Fluorescence images of hMSCs exhibited acceptable transport efficiency of CP26a into hMSCs cells.

Next, we quantified the uptake efficiency of CCMV, Lipofectamine2000-miR-26a (lipo26a), and CP-miR-26a (CP26a) *via* flow cytometry (Fig. 2B). The peak of cells treated with CCMV-Atto647 was shifted to the right side compared to the negative control group (hMSCs without any further treatment), which indicated that hMSCs could absorb CCMV. A similar tendency was observed in lipo26a-CY3 and CP26a-CY3 groups, and the positive cell proportion of lipo26a and CP26a was at a comparable level (84.0% *versus* 94.1%). Taken together, CP26a could be taken in by hMSCs efficiently and localized in the cytoplasm, while the lipo26a had relatively lower efficiency to access hMSCs.

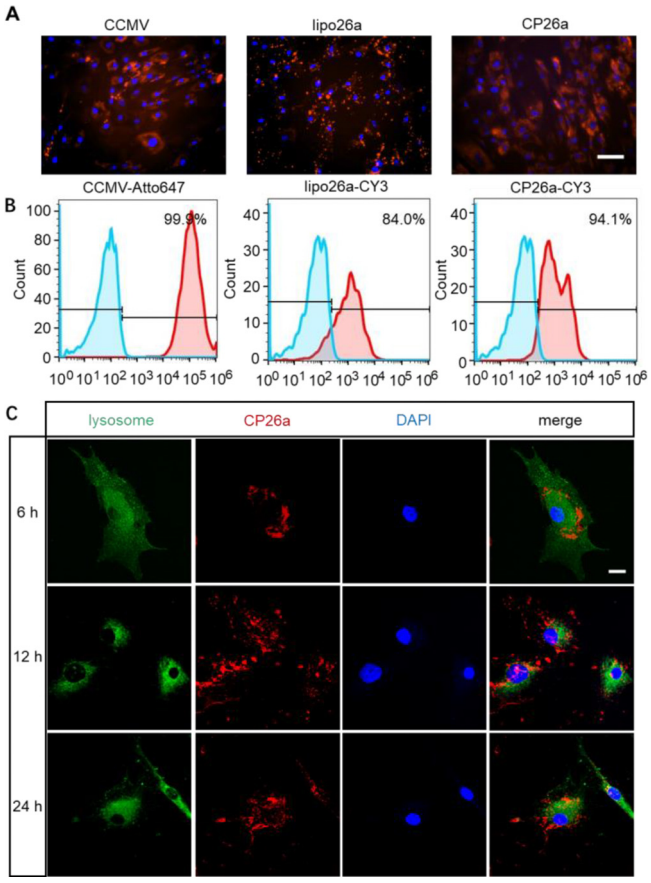

Fig. 2. Internalization of CCMV, lipo26a, and CP26a by hMSCs. (A) Fluorescence microscope images of hMSCs treated with CCMV, lipo26a, and CP26a for 72 h (Scale bar = 100 μm). (B) Flow cytometry was used to detect cellular uptake efficiency of CCMV, lipo26a, and CP26a by hMSCs after treatment for 72 h. (C) Confocal laser scanning microscopy (CLSM) images of hMSCs treated with CP26a for 6 h, 12 h, and 24 h were taken to study the lysosome escape (Scale bar = 20 μm; Red: miR-26a/CCMV, Blue: nucleus, Green: lysosome).

To further study the location of miR-26a, hMSCs were incubated with CP26a-CY3 at a concentration of 100 nmol/L. CLSM images were taken at different incubation time points. As shown in Fig. 2C, after incubation for 6 h, red fluorescence was observed in the cytoplasm, and overlapped with the green fluorescence of the lysosome, suggesting that CP26a has entered the cell and internalized with the lysosome. Following the incubation for 12 h, red fluorescence was partially separated from green fluorescence and dispersed in the cytoplasm, whereas red fluorescence was observed throughout the cytoplasm for 24 h, suggesting the successful release of miR-26a from the lysosome. This is in line with a previous study of CCMV uptake pathways by Mark *et al.*, where they claimed that CCMV was taken into cells through the endocytosis pathway followed by internalization with lysosome and ultimate escape from lysosome [32].

Plant viruses have the potential to be novel gene delivery systems as they are noninfectious to mammals, thereby with no risk of gene integration. Likewise, as a traditional gene transfection system, Lipofectamine2000 has been widely applied. It can pack the negatively charged nucleotide with a positively charged lipid membrane by electrostatic interaction to form a nucleotide-liposome complex and infiltrated it into the cell membrane by endocytosis.

However, high-dosage liposomes could cause great cytotoxicity to cells resulting from hydrophilic headgroups [36], the large size, and the highly positively charged surface of cationic lipids [37]. To compare the cytotoxicity of CCMV-CP and Lipofectamine2000,

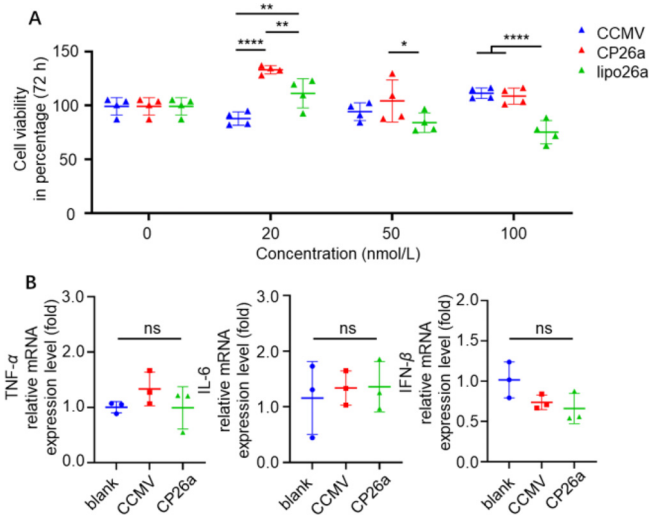

Fig. 3. (A) Cellular proliferation of hMSCs treated with CCMV, lipo26a and CP26a for 72 h (detected by CCK-8 assay). (B) qPCR analysis of TNF-α, IFN-β and IL-6 expression levels of RAW264.7 incubated with CCMV and CP26a after 6 h. * $P < 0.05$; ** $P < 0.01$; *** $P < 0.001$; **** $P < 0.0001$; ns: no significance.

hMSCs were treated with CCMV, lipo26a, and CP26a at various concentrations (0, 20, 50, 100 nmol/L) for 24, 48, and 72 h. The CCK-8 assay results revealed that lipo26a caused significant cytotoxicity at the concentration of 100 nmol/L, which is a recommended biofunctional dosage of miR-26a to induce mesenchymal stem cells osteogenesis to hMSCs. At 24 and 48 h, the proliferation of cells treated with lipo26a has been restrained greatly (Fig. S3 in Supporting information). The inhibition effect on cell growth was also detected after incubation for 72 h (Fig. 3A). The relative cell viability of hMSCs in the 100 nmol/L lipo26a group was 57.59% at 24 h, 72.69% at 48 h, and 75.19% at 72 h respectively. Furthermore, no significant cytotoxicity of CCMV or CP26a was detected. The medium of CCMV and CP26a group was not refreshed before the cell viability assay. This part of results shows that CCMV-CP had no adverse effect on hMSCs proliferation and exceed Lipofectamine2000 in the field of biocompatibility, providing a promising way to build a novel plant viral gene delivery platform.

We also detected monocyte/macrophage immune response toward CCMV and CP26a. After treating RAW264.7 cells with CCMV and CP26a for 6 h, the mRNA expression level of TNF-α, IFN-β and IL-6 was measured. As shown in Fig. 3B, there was no significant change in the mRNA expression level of TNF-α, IFN-β, and IL-6, indicating that CCMV or CP26a did not cause a severe immune response. Sourabh *et al.* [38] performed experiments focusing on the potency of Cowpea mosaic virus (CPMV) to trigger anti-tumor immunity as a vaccine. They compared several plant viruses' ability to elevate pro-inflammatory cytokines and concluded that CPMV could significantly promote the expression of IL-6 and IFN-γ (promotes recruitment of immune cells into the tumor microenvironment and induces Th-1 anti-tumor immunity), while the level of IL-10 (alleviate immunosuppression which leads to immunotherapies resisted) was decreased. On the contrary, CCMV did not perform outstandingly since it caused no significant impact on IL-10 and IFN-β expression levels. Our result is in line with Sourabh's observation.

To further study the release of miR-26a from CP26a *in vitro*, hMSCs were incubated with CP26a at a concentration of 100 nmol/L miR-26a, the level of miR-26a released at different incubation time points was analyzed by qPCR experiments (Fig. S4 in Supporting information). The expression level of miR-26a both in the lipo26a and CP26a group were significantly increased com-

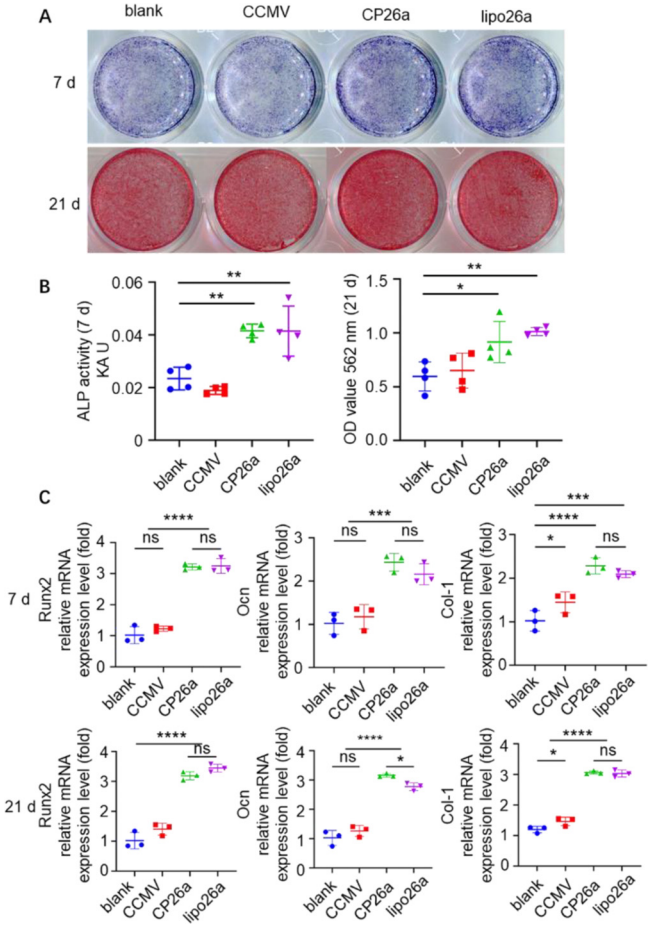

Fig. 4. Osteogenesis of hMSCs induced by CCMV, lipo26a, and CP26a. (A) ALP and ARS staining of hMSCs treated with CCMV, lipo26a, and CP26a for 72 h and incubated in osteogenic medium. (B) ALP activity and mineralization nodules of hMSCs treated with CCMV, lipo26a, and CP26a for 72 h and incubated in osteogenic medium. (C) qPCR analysis of Runx2, Ocn, and Col-1 osteogenic gene expression levels of hMSCs treated with CCMV, lipo26a, and CP26a for 72 h and incubated in osteogenic medium. * $P < 0.05$; ** $P < 0.01$; *** $P < 0.001$; **** $P < 0.0001$; ns: no significance.

pared with that of the blank group, there was no significant difference between the blank group and CCMV group. Accumulated release of miR-26a from the CP26a group was found after incubation for 72 h, suggesting good delivery efficiency of CP26a.

The increase in ALP activity was defined as a marker of early osteogenic differentiation towards mature osteoblasts [39]. Calcium nodules were produced during the late stage of osteogenesis [5]. Thus, to investigate whether CP26a could release miR-26a and promote osteogenesis, activity assays of ALP and ARS were performed after osteogenic induction. Fig. 4A revealed that CP26a and lipo26a groups exhibited the highest ALP intensity compared with blank and CCMV groups. Meanwhile, native CCMV did not cause any promotion effects on osteogenesis. The quantity assay revealed that ALP activity in CP26a and lipo26a groups displayed a 2-fold increase compared with blank and CCMV groups, which is in line with the staining results (Fig. 4B). A vast number of mineralized nodules were observed in CP26a and lipo26a groups according to the ARS staining results. The quantification of mineralized nodules also showed the superiority of CP26a and lipo26a over other groups (Figs. 4A and B). This part of the results indicated that CP26a had a comparative induction effect on osteogenesis with lipo26a.

Since osteogenesis phenotype induced by CP26a and lipo26a has been observed, we tried to uncover the mechanisms. Previous studies have revealed that miR-26a could specifically inhibit GSK-3β protein, subsequently inhibit β-catenin phosphorylation and active Wnt signaling pathway to promote osteogenic differentiation of MSCs, which ultimately resulted in bone regeneration. Runx2 is a transcription factor involved at the initial stages of osteoblast differentiation, which regulates some important proteins related to osteogenesis. In addition, Col-1 plays an important role in the maturation and mineralization of the bone matrix, and it is an early-stage marker of osteoblast differentiation. Moreover, Osteocalcin (Ocn) is expressed at the late stage of osteoblast differentiation and it is involved in the process of cell adhesion, proliferation, and extracellular matrix. Thus, the expression level of these three representative osteogenic regulation genes was analyzed and shown in Fig. 4C. hMSCs treated with CP26a and lipo26a exhibited an increase in levels of Runx2, Ocn, and Col-1 after osteogenic induction on both the 7^{th} and 21^{st} days. There was no significant difference between CCMV and blank groups. This result indicates that CP26a could efficiently promote the expression of osteogenic regulated genes in hMSCs.

The physiological roles of miR-26a on the osteogenesis regulation of MSCs have been widely reported. However, the main obstacles for miR-26a to be applied to bone regeneration therapy come from its instability under physiological conditions and low cell membrane penetration capability. Cowpea chlorotic mottle virus, owning to its advantages of noninfectious to mammals, great biocompatibility, and passive transporting through cells, appears to have great prospects for development as a gene delivery platform. Here we successfully built a novel vector by packing miR-26a with CCMV-CP and examined its potential in protecting and transporting nucleotides into cells. What needs to be emphasized is that we packed double-stranded miRNAs in this experiment, considering short single-stranded miRNAs were extremely unstable *in vitro* and prone to be degraded during preparation. Even though the native genomic ssRNA was replaced by miR-26a, the essential characteristic of reassembled VLPs did not change. What is more, CP could protect miRNA from degrading under storage situations for a relatively long term. In a series of experiments focusing on biomaterials application *in vitro*, CP26a could be taken into hMSCs efficiently and showed no cytotoxicity to hMSCs. On the contrary, lipo26a inhibited hMSCs proliferation significantly. As for bioactivity assay, both CP26a and lipo26a could promote osteogenic differentiation of hMSCs both at the early and late stages of osteogenesis. The possibility of CP dimers inducing osteogenesis was also excluded since CCMV treatment did not contribute to positive results, confirming valid delivery of miR-26a by CCMV-CP.

Unlike other gene delivery systems, such as the liposome system, which was prepared before cell treatment immediately, CCMV-CP packed nucleotide could be produced several days ahead of use, making it more convenient. We also certified the structure of CP26a remained stable 30 days after preparation. In a word, plant virus CCMV is feasible to serve as a novel gene delivery system with its superiority of higher biocompatibility than Lipofectamine2000 reagent.

Viruses are natural vehicles for the delivery of genes, numerous works have been carried out to investigate the full potential of CCMV as gene vectors. Cai *et al.* [29] have used CCMV VLPs carrying CpG ODN to inhibit tumor growth *via* enhanced uptake by tumor-associated macrophages. Attempts of delivering siRNA and mRNA into mammalian cells by CCMV have also been reported [26,28], CCMV exhibited excellent cellular uptake efficiency. Here, it is the first time for us to deliver miR-26a into hMSCs with favorable transfection efficiency and both low cytotoxicity and immune response. However, an in-depth study is still required to understand the lysosome escape mechanism, and thereafter *in vivo* experiments could be carried out.

Declaration of competing interest

We wish to confirm that there are no known conflicts of interest associated with this publication and there has been no significant financial support for this work that could have influenced its outcome. We confirm that the manuscript has been read and approved by all named authors and that there are no other persons who satisfied the criteria for authorship but are not listed. We further confirm that the order of authors listed in the manuscript has been approved by all of us. We confirm that we have given due consideration to the protection of intellectual property associated with this work and that there are no impediments to publication, including the timing of publication, with respect to intellectual property. In so doing we confirm that we have followed the regulations of our institutions concerning intellectual property.

Acknowledgments

This work was supported by the research funding from West China School/Hospital of Stomatology, Sichuan University (Nos. RCDWJS2021-15, RD-03-202010, RD-02-202004), the research funding from the State Key Laboratory of Oral Diseases (No. SKLOD202111), and the fellowship of China Postdoctoral Science Foundation (No. 2020TQ0211). We thank Prof. Dr. X. Zhu from the College of Life Sciences, Sichuan University for the FPLC measurement and Ceshigo Research Service for the TEM measurement.

Supplementary materials

Supplementary material associated with this article can be found, in the online version, at doi:10.1016/j.cclet.2022.04.046.

References

[1] H.C. Pape, A. Evans, P. Kobbe, J. Orthop. Trauma 24 (Suppl. 1) (2010) S36–S40.
[2] L. Zhang, G. Yang, B.N. Johnson, X. Jia, Acta Biomater. 84 (2019) 16–33.
[3] H.J. Haugen, S.P. Lyngstadaas, F. Rossi, G. Perale, J. Clin. Periodontol. 46 (Suppl. 21) (2019) 92–102.
[4] R. Dimitriou, E. Jones, D. McGonagle, P.V. Giannoudis, BMC Med. 9 (2011) 66.
[5] Y. Yan, H. Chen, H. Zhang, et al., Biomaterials 190-191 (2019) 97–110.
[6] K.W. Ko, S.Y. Park, E.H. Lee, et al., ACS Nano 15 (2021) 7575–7585.
[7] Y. Okuchi, J. Reeves, S.S. Ng, et al., Nat. Mater. 20 (2021) 108–118.
[8] T. Cui, J. Yu, Q. Li, et al., Adv. Mater. 32 (2020) e2000982.
[9] Y. Wang, C. Li, L. Du, Y. Liu, Chin. Chem. Lett. 31 (2020) 275–280.
[10] S. Guo, B. Liu, M. Zhang, et al., Chin. Chem. Lett. 32 (2021) 102–106.
[11] Y. Zhang, L. Wang, J. Wang, S. Xin, X. Sheng, Chin. Chem. Lett. 32 (2021) 1902–1906.
[12] M. Nakashima, A.H. Reddi, Nat. Biotechnol. 21 (2003) 1025–1032.
[13] J. Min, K.Y. Choi, E.C. Dreaden, et al., ACS Nano 10 (2016) 4441–4450.
[14] L. Li, W. Liu, Y. Zhao, et al., ACS Appl. Mater. Interfaces 12 (2020) 3474–3493.
[15] H. Xing, X. Wang, G. Xiao, et al., Biomaterials 235 (2020) 119784.
[16] X. Zhang, Y. Li, Y.E. Chen, J. Chen, P.X. Ma, Nat. Commun. 7 (2016) 10376.
[17] L.F.R. Gebert, I.J. MacRae, Nat. Rev. Mol. Cell Biol. 20 (2019) 21–37.
[18] X. Su, L. Liao, Y. Shuai, et al., Cell Death. Dis. 6 (2015) e1851.
[19] E.K. Tsekoura, R.B. K.C., H. Uludag, ACS Biomater Sci. Eng. 3 (2017) 1195–1206.
[20] J. Yan, X. Lu, X. Zhu, et al., Int. J. Nanomed. 15 (2020) 497–511.
[21] Z. Liu, H. Chang, Y. Hou, et al., Mol. Med. Rep. 18 (2018) 5317–5326.
[22] K.L. Lee, B.L. Carpenter, A.M. Wen, R.A. Ghiladi, N.F. Steinmetz, ACS Biomater. Sci. Eng. 2 (2016) 838–844.
[23] M.A. Bruckman, A.E. Czapar, A. VanMeter, L.N. Randolph, N.F. Steinmetz, J. Control. Release 231 (2016) 103–113.
[24] C.E. Franke, A.E. Czapar, R.B. Patel, N.F. Steinmetz, Mol. Pharm. 15 (2018) 2922–2931.
[25] A.M. Wen, K.L. Lee, P. Cao, et al., Bioconjug. Chem. 27 (2016) 1227–1235.
[26] O. Azizgolshani, R.F. Garmann, R. Cadena-Nava, C.M. Knobler, W.M. Gelbart, Virology 441 (2013) 12–17.
[27] S.J. Maassen, The Assembly and Confinement Properties of the Cowpea Chlorotic Mottle Virus, PhD Thesis, University of Twente, Enschede, 2018.
[28] P. Lam, N.F. Steinmetz, Biomater. Sci. 7 (2019) 3138–3142.
[29] H. Cai, S. Shukla, N.F. Steinmetz, Adv. Funct. Mater. 30 (2020) 1908743.

[30] I.J. Minten, L.J.A. Hendriks, R.J.M. Nolte, J.J.L.M. Cornelissen, J. Am. Chem. Soc. 131 (2009) 17771–17773.
[31] M. Manchester, P. Singh, Adv. Drug. Deliv. Rev. 58 (2006) 1505–1522.
[32] M.V. de Ruiter, R.M. van der Hee, A.J.M. Driessen, et al., J. Control. Release 307 (2019) 342–354.
[33] J.P. Michel, M. Gingery, L. Lavelle, J. Virol. Methods 122 (2004) 195–198.
[34] D. Luque, J.R. Castón, Nat. Chem. Biol. 16 (2020) 231–239.
[35] S.J. Maassen, M.V. de Ruiter, S. Lindhoud, J.J.L.M. Cornelissen, Chemistry 24 (2018) 7456–7463.
[36] Y. Zhu, Y. Meng, Y. Zhao, et al., Colloids Surf. B: Biointerfaces 179 (2019) 66–76.
[37] H. Lv, S. Zhang, B. Wang, S. Cui, J. Yan, J. Control. Release 114 (2006) 100–109.
[38] S. Shukla, C. Wang, V. Beiss, et al., Biomater. Sci. 8 (2020) 5489–5503.
[39] X. Chen, L. Wang, K. Zhao, H. Wang, Tissue Eng. Part B: Rev. 24 (2018) 215–225.